INS--956

JP9306095

INSTITUTE FOR NUCLEAR STUDY
UNIVERSITY OF TOKYO
Tanashi, Tokyo 188
Japan

INS-Rep.-956
Dec. 1992

A NEW COOLING AND FOCUSING DEVICE FOR ION GUIDE

HONG JIE XU[1], MICHIHARU WADA, JINICHI TANAKA,
HIROKANE KAWAKAMI and ICHIRO KATAYAMA
Institute for Nuclear Study, the University of Tokyo
and
SHUNSUKE OHTANI
Institute for Laser Science, the University of Electro-Communication

A NEW COOLING AND FOCUSING DEVICE FOR ION GUIDE

HONG JIE XU[1], MICHIHARU WADA, JINICHI TANAKA,
HIROKANE KAWAKAMI and ICHIRO KATAYAMA
Institute for Nuclear Study, the University of Tokyo
and
SHUNSUKE OHTANI
Institute for Laser Science, the University of Electro-Communication

Abstract: A highly efficient focusing device using RF multipole field "sextupole-ion-beam-guide (SPIG)" has been developed for the ion guide isotope separator on-line (IGISOL). The SPIG, placed after the nozzle, consists of the six circular rods uniformly distributed on a circle in the plane perpendicular to the symmetry axis. Under the combined action of the sextupole RF electric field produced by the rods and helium gas flow, a good focusing and cooling of ions from the Ion Guide with highly efficient transmission are achieved in the SPIG. The experimental results using a discharge ion source show that almost nearly 90 % of the ions out of the nozzle can be transported through the SPIG, and the width of the kinetic energy distribution after the SPIG is about 0.8 eV (FWHM). These experimental results coincide well with the Monte-Carlo simulation results and the simulation also predicts the size of the spatial distribution in the plane perpendicular to the symmetry axis is smaller than 1 mmΦ at the end of the SPIG.

---

[1] On leave from the Institute of Nuclear Research, ACADEMIA SINICA, Shanghai.

1. Introduction

The on-line isotope separator (ISOL) has played an important role in studies of short-lived unstable nuclei [1,2]. Comparing with the normal ISOL equipped with ion sources, the ion-guide isotope separator on-line (IGISOL) developed by Ärje et al. [3,4] has advantages that it works very stable for all elements because no "ion source" is used, and that it can be applied to radioactivities with short half-lives down to $t_{1/2}$ = 0.1 ms. The operational principle of the ion guide in IGISOL is based on thermalization of primary recoil ions in helium gas in singly charged state and on subsequent transfer of ions by helium gas flow through a differential pumping system into the acceleration stage of a mass separator. An ideal ion guide should be that in which all kind of ions with any kinetic energy can be efficiently thermalized and transmitted through a differential pumping system with the kinetic energy and spatial spread as small as possible.

Recent works have improved the original type of IGISOL; Nomura et al. [5] extended the application of IGISOL to be used after a gas-filled recoil isotope separator (GARIS). This can eliminate the recombination of ions in plasma produced by the primary beam in He gas. Iivonen et al. [6] have developed the squeezer ion guide (squeezer) with one or more ring grids at low electric potential in the space between nozzle and skimmer. They achieved a transmission efficiency of 75 % (the ratio between the yield through nozzle and that through skimmer) and the width of the kinetic energy distribution of 2.5-3.5 eV.

An ion trap system to perform high resolution laser spectroscopy of unstable nuclei has been being developed at

Institute for Nuclear Study (INS), the University of Tokyo [7,8]. Heavy ion beams from the INS SF cyclotron will be used to produce unstable nuclei. The recoil products of the unstable nuclei are separated and collected by the GARIS. As the unstable nuclear beam from the GARIS has generally a broad kinetic energy distribution as well as a large emittance; it is difficult to capture even a small fraction of ions directly by the ion trap. It is, then, indispensable to reduce the phase space volume of the beam. To this purpose an ion guide is placed at the focal plane of the GARIS, in which the unstable nuclear ions are thermalized in helium gas and extracted with a helium gas flow through a nozzle. Some focusing devices for the ions will be required close to the nozzle. The ions extracted and focussed by the device, then transported through a beam guide [9], will be injected into a RF trap for laser spectroscopy.

In this paper a highly efficient focusing device for ions from the nozzle, developed at INS, is described. The grids and skimmer after nozzle used in the squeezer [6] were replaced by the six rods which pass through a plate used as a skimmer. The six rods are uniformly distributed on a circle in the plane perpendicular to the symmetry axis, called sextupole-ion-beam-guide (SPIG), on which a radio-frequency (RF) electric field is applied.

The SPIG has been experimentally tested off-line with an arc discharge ion source and also the properties of the SPIG have been examined by a Monte-Calro simulation. The experimental results show that under the optimum working conditions almost all of the ions from the nozzle can pass the SPIG with a small kinetic energy spread of 0.8 eV (FWHM). Those experimental results coincide with the Monte-Calro simulation and the simulation also predicts

the size of the spatial distribution in the plane perpendicular to the symmetry axis is smaller than 1mmϕ at the end of the SPIG. It should be noted that the ion beam guide using a multi-pole RF electric field has been developed for low energy ion-atom collision study by Okuno [9]. In the present work this has been successfully applied to the ion guide system with IGISOL even under poor vacuum.

2. Principle of the SPIG

A schematic layout of the ion guide is shown in Fig. 1, which includes a helium gas chamber to produce ions by an arc discharge ion source. In the case of on-line work, ions are injected from outside through a mylar entrance window. An energy degrader is placed in front of the entrance window to slow down ions so that the ions after passing through it could just stop inside the helium gas chamber. Ions at thermal temperature are hard to be neutralized in helium gas, because the ionization energy of a helium atom is too high for ions to pick up an electron from the helium atom. The helium gas pressure is several tens kPa. Under this pressure ions with thermal energy have a mean free path of around 1×10^{-6} m, they are, therefore, completely driven by helium gas flow. Ions are accelerated in the nozzle by helium gas expanding through to a typical kinetic energy of the order of magnitude of 0.1 eV.

The SPIG is placed so close to the nozzle that almost of all ions are injected into the SPIG by the helium jet on leaving the nozzle of the gas chamber. In the SPIG most of helium gas are evacuated out through the space between the electrodes. There is, however,

not negligible part of helium gas which can pass through the SPIG, because the helium gas enters the SPIG in the form of a shock wave. Ions in the SPIG are subject to two forces, namely those from the RF electric field produced by the six electrodes and from the helium gas flow field produced by surviving helium gas.

The potential around the central axis produced by parallel 2N rods supplied with RF voltages of $V_{rf}\cdot\cos(\omega t)$ of opposite phase, is represented by

$$U = (r/\rho)^N V_{rf}\cos(N\theta)\cdot\cos(\omega t). \qquad (2.1)$$

Here r and θ are cylindrical coordinates, z being the symmetry axis, ρ the radius of the inscribed circle formed by rods, t the time, and V_{rf} the amplitude of the RF voltage with a frequency of $\omega/2\pi$. For the case of N = 3 (i.e, sextupole), the potential is given by

$$U = V_{rf}(r/\rho)^3\cdot\cos(3\theta)\cdot\cos(\omega t), \qquad \text{in cylindrical coordinate,}$$

or

$$U = V_{rf}(\cos(\omega t)/\rho^3)\cdot(x^3-3xy^2), \qquad \text{in Cartesian coordinate,}$$

where, the axes are defined as shown in Fig.1. The above potential shows that the RF electric field in the SPIG only affects the radial motion of charged particles and never affects the drift motion along the z-axis of the SPIG.

In the sextupole RF field, the trajectory of singly charged ions projected on the x-y plane can be formulated by the following differential equations;

$$d^2x/dt^2 = 3\cdot(V_{rf}\cos(\omega t)/m\rho^3)\cdot(x^2-y^2), \quad \text{and}$$

(2.2)

$$d^2y/dt^2 = 6\cdot(V_{rf}\cos(\omega t)/m\rho^3)\cdot xy,$$

where m is the mass of the particle.

Employing the following substitution,

$$T = \omega t, \quad R = r/\rho \quad \text{and} \quad A = 3V_{rf}/(m\rho^2\omega^2),$$

the equations (2.2) can be transformed to the following normalized, dimensionless differential equations,

$$\begin{aligned} &d^2R/dt^2 - Rd^2\theta/dt^2 = -AR^2\cos(3\theta)\cdot\cos T, \\ &Rd^2\theta/dt^2 + 2dr/dt\cdot d\theta/dt = AR^2\sin(3\theta)\cdot\cos T, \text{ and} \\ &dz/dt = 0. \end{aligned} \tag{2.3}$$

Although it is difficult to get an exact solution of the differential equation (2.3), under a certain approximation we can get the solution [9,10]. The radial motion of the particle in the solution can be separated into two parts; namely, the fast oscillatory part and the slow average part. When the frequency ω is high enough, the fast oscillatory part becomes negligible and the slow average part becomes close to an exact trajectory. The average trajectory can be described by an ordinary periodic motion under a conserved force of the effective potential U_{eff},

$$\begin{aligned} Ueff &= 9(r^4V_{rf}^2)/(4m\omega^2\rho^6) \\ &= 3V_{rf}AR^4/4. \end{aligned} \tag{2.4}$$

The concept of the effective potential is useful in understanding the physical characteristics of the SPIG. From equation (2.4), we can see the relationship between the depth of the potential well and the parameters of the SPIG, such as V_{rf}, ω and ρ.

The numerical computer-simulation is another useful method to solve the differential equations (2.3). A trajectory of moving O_2^+ ion in the SPIG from a computer simulation is shown in Fig. 3, where $\omega/2\pi$ is 4.721 MHz and V_{rf} is 60 volt. From this figure we can see that the amplitude of the fast oscillation is much smaller than that of the slow average motion.

The helium gas issuing freely from the nozzle creates a highly underexpanding supersonic jet, and the pressure in the nozzle is thought to be equal to the pressure in the gas chamber. This pressure is much higher than the ambient ones. Iivonen et al. [6] have reported that the high pressure part of the shock wave is extending in the region of 2 - 3 mm from the nozzle, and then the pressure rapidly reduces to an almost constant low pressure.

According to the properties of the flow field of helium gas discussed above, the interaction between flow field and ions could be understood qualitatively as follows. In the region near the nozzle, ions are driven mainly by gas flow along the axis which is the direction of the movement of the shock wave. In the region where the shock wave becomes negligible, the "flow field" can be separated into the random thermal motion of individual gas molecule and the collective flow. The former could cool ions if the ion energy is higher than the thermal one and makes the ions diffuse in gas. The latter would work either transporting ions through the SPIG or bringing ions out of the SPIG.

In practice, the SPIG is supplied not only with V_{rf}, but also with several DC voltages, i.e., a gas chamber voltage V_g and an average potential V_m on the SPIG. It is, however, not so clear how the potential difference V_m - V_g may work to accelerate ions at the nozzle position. This is really one of our major interest in the present work. This has been examined not only experimentally, but also in the simulation work, which will be discussed in the next section.

3. Result and discussion

3.1. Experiment

The SPIG has been tested off-line with a discharge ion source placed in the He gas chamber at INS. The apparatus used in this experiment is shown in Figs. 1 and 2 (photograph). Helium gas is introduced through a variable leak valve into the gas chamber. The gas chamber consists of a cylindrical vessel of 65 mmϕ and 60 mm length and a half sphere with a nozzle of 1.2 mmϕ at the end. The arc electrodes for ion source are located near the nozzle in the vessel. The commercially available helium gas was used in the experiment for producing, stopping and transporting ions of impurity gas. From the measurements of mass spectra [11] we can assume that most of the ions are O_2^{+*}. The O_2 gas was contained in the He gas as an impurity with a fraction of ppm order.

The SPIG, placed after the nozzle, extends through a plate of 30 mm thick which separates two chambers with different vacuum

---

* According to ref. [11] the dominant ions extracted are O^+, under the applying the skimmer potential of 500 volts. In the present case, however, we apply only 10 volts or less, so we speculate that almost all O_2^+ ions don't dissociate.

systems. The SPIG consists of six molybdenum rods of 1mmϕ and 100 mm length, which are uniformly distributed on a circle of 3.5 mmϕ in the plane perpendicular to the symmetry axis and are supplied with a RF voltages of $V_{rf}\cdot\cos(\omega t)$ alternatively in opposite phases.

The pressure of gas chamber was 10 kPa. The first vacuum chamber next to the gas chamber was connected to a combination of mechanical boosters of 4200 and 1200 m^3/h and a rotary pump of 5000 *l*/min. Helium gas can flow out from the space between the electrodes of the SPIG, and then is evacuated by the pumps. During the measurement the pressures of the two chambers separated by a skimmer plate were 80 Pa and 13 Pa, respectively. A Farady cup was placed 10 mm downstream from the end of the SPIG to collect the ions having passed the SPIG. The skimmer plate is also insulated to measure the current of scattered ions.

The properties of the SPIG were measured, and the results are shown in Figs. 4(a) and 5. Fig. 4(a) is the relation between the transmission current of the SPIG with the RF voltage V_{rf} for the case V_m = 10 V, V_g= 15 V and $\omega/2\pi$ = 4.721 MHz. The black circle represents the ion current to the Farady cup (FC) and the white circle is the one to the skimmer. The current to the SPIG rods was not measured. In Fig. 4(a) the transmission current after the SPIG vs. the voltage is shown. The parameters for this measurement were V_g = 10 V, V_{ac} = 60 V and $\omega/2\pi$ = 4.721 MHz. In these measurements, the total current from the gas cell was about 25 nA which is the sum of the currents collected on the skimmer plate and the SPIG rods while the RF was off. The current to the FC was negligible. The maximum current of 28 nA in Fig. 4(a) is a little bit larger than 25 nA. This small difference of the two currents is

supposed to be due to the instability of the ion source used. In Fig. 5, at the maximum current to the FC, there is a leaking current of 10 % of the FC current to the skimmer plate. So the maximum transmission is about 90 %. The threshold and rapid increase in the yield after the SPIG in Fig. 5 give the information about the kinetic energy distribution of the ions. From the dotted line shape in Fig. 5, the energy spread was analyzed to be less than 0.8 e V (FWHM).

3.2. Monte-Carlo simulation

The property of the SPIG has been simulated by the Monte-carlo calculation. The trajectory for each individual ion has been traced step by step until it escapes from the SPIG or reaches at the end of the SPIG. In the simulation, the effects of the RF electric field and the helium flow field on ions were calculated separately. The motion of ion under the RF electric field can be obtained by solving the differential equation (2.3) with the stepwise integration method, i.e., the Runge-Kutta method. The time step (t_d) must be small enough to guarantee that the simulated trajectory is very close to the exact one; the ratio (T/t_d) of the period (T) of the RF electric field to the time step was empirically chosen to be 500-1000 depending on different RF voltage V_{rf} in this simulation. It is noted that in the present calculation the space charge effects were not considered.

The interaction between the gas flow and the ion can be represented as the collisions of the ion with gas atoms calculated by the rigid sphere model (RS). The RS model takes three assumptions. In the first place the rigid sphere potential is used as

the interaction between the ion and the gas molecule and the inner freedom of the gas molecule is neglected. In the second place the collision probability between two successive collisions with the distance L is assumed to follow the exponential distribution, $\exp(-L/L_{bar})$, where L_{bar} is the mean free path of ions and is inversely proportional to the pressure. In the third place the velocities of thermal motion of gas atoms follow the Maxwell-Boltzman distribution at the room temperature. Under the first approximation, the change of the pressure along the z-axis of the SPIG, was assumed decreasing linearly with z, which means that L_{bar} increases linearly with z. The collective translational motion along the z direction is represented by a constant drift velocity, which is of the order of magnitude of the speed of sound of the helium gas, a typical value being 0.01 eV. The rotational motion was neglected because the energy transfer to ions due to this gas flow is much less than that given by the RF acceleration. The ions are assumed to be randomly generated with the velocities, order of 0.1 eV, within a round area having the same diameter as the nozzle. They are ejected from the disk in the forward direction within 2π solid angle.

The dependence of the transmission efficiency on the RF voltage according to the computer simulation for the case of O_2^+ ions with $\omega/2\pi$ = 4.721 MHz is shown in Fig. 4(b). In this simulation the initial velocity of ions includes a random part of 0.1 eV, an alignment part of 5 eV, and the translational kinetic energy of gas flow 0.01 eV. The total number of ion is 200 for each V_{rf}. The experimental and calculated curves agree very well with each other. When the ions move in the SPIG, the changes of their mean kinetic energy and the mean distance r from z axis of the SPIG are

shown in Fig. 6, where V_{rf} is 60 V and other parameters are the same as in Fig. 4(b). These curves are the average for 40 ions. The rapid cooling effect of ions by the collisions with the gas atoms can be seen. Fig. 7 shows the kinetic energy (E) and position (r) distributions of the ion at the end of the SPIG under the same conditions as in Fig. 6. We can see that the most of the ions are distributed inside a circle with radius of 0.5 mm in x - y plane and have a kinetic energy of 0.1 - 0.3 eV, which explains the experimental results in Fig. 5 rather well.

3.3. Discussion

Of the three assumptions in the RS model used in the simulation calculation, the first one of the rigid sphere potential might be too simple. Considering the polarization of the gas atoms when an ion approaches it, there should be the interaction of $1/r^4$ between them, where r denotes the distance between the molecule and the ion. Another more complicate potential, which takes into account this polarization effect and is called the Morse-Splind-van der Vaals potential (MSV) [12], has been also tried in our simulation calculation. The results of the MSV potential have hardly shown any difference from the results of the RS model; the MSV model took much more computer time than the RS model. Most of calculation was, therefore, done using the RS model. A similar conclusion has also been obtained in the "direct" Monte-Carlo simulation of strong shock wave by Bird [13]. The second assumption of the RS model is different from the assumption that the collision probability for an ion with the time interval t between two successive collisions follows the exponential distribution, exp(-

t/t_{bar}), where t_{bar} is the mean free time of ion. This model has been employed in our previous papers [7,8]. The advantage of RS model in the present case is that change of the pressure effect is easily implemented. The $\exp(-t/t_{bar})$ distribution model is effective in the case of a constant gas pressure, for example in the calculation of ions in an RF trap. The choice of the drift velocity of gas molecules has been found to have no influence on the transmission efficiency of the SPIG in a wide range of 0.001 - 0.5 eV. But for gas molecules with higher drift velocity, the kinetic energy of ions has been found to become higher, which is quite reasonable. The more details of discussion about the simulation will be given in ref. 14.

The small difference in pressure between the two chambers used in this experiments is a deficiency for the requirements of IGISOL. We are, thus, preparing a new SPIG with a smaller radius so as to reduce the conductance. It is also possible to put another skimmers and chambers to improve the vacuum to the UHV region.

As a conclusion, the SPIG ion-guide will be very useful in order to inject ions directly into an ion-trap, in particular, for unstable nuclear beams from a recoil mass separator as well as to an IGISOL for improving the beam quality.

Acknowledgement

We are deeply grateful to Prof. K. Okuno for his helpful comments and discussions on the SPIG, and to Prof. M. Fujioka for reading this manuscript. We also thank the Nuclear Physics Division staffs for their warm support of this project. One of the

authors (H. J. Xu) would like to thank the Inoue Foundation for the support of his stay in Japan and to Prof. T. Yamazaki for his encouragement.

References

[1] E. Roeckl, Nucl. Phys. A400(1983)131c.

[2] R. Kirchner, Nucl. Instr. and Meth. 186(1981)275.

[3] J. Ärje et al., Phys. Rev. Lett. 54 (1985) 99 .

[4] J. Ärje et al., Nucl. Instr. and Meth. A247 (1986) 431.

[5] T. Nomura et al., Nucl. Instr. and Meth., A269(1988)23.

[6] A. Iivonen, K. Riikonen, R. Saintola, K. Valli and K. Morita, Nucl. Instr. and Meth. A307(1991)69.

[7] I. Katayama et al., Nucl. Instr. and Meth. B70(1992)509.

[8] M. Wada, Physica Scripta 46(1992); in printing.

[9] K. Okuno, J. Phys. Soc. Japan 55(1986)1504.

[10] H. Dehmelt, Adv. At. Mol. Phys. 3(1967)53.

[11] M. Yoshii, thesis of Tohoku University, 1986, unpublished.

[12] P. E. Siska, J. Chem. Phys. 71(1979)3942.

[13] G. A. Bird, Progr. in Astro. and Aero., 74(1981)239.

[14] H. J. Xu et al., INS Report; to be published.

Figure Captions

Fig. 1. Layout of the apparatus used in the present experiment and the direction of coordinates.

Fig. 2. Photograph of the gas chamber with a nozzle and the SPIG.

Fig. 3. The trajectory of an O_2^+ ion in the SPIG with no gas collision for the case of V_{rf} = 60 V and $\omega/2\pi$ = 4.721 MHz. The initial velocities V_x, V_y and V_z are 284, 284 and 5671 m/s respectively, and the initial position is x = -0.6 mm and y = 0 mm. (a) shows the projected orbits on the x-y plane, and (b) trajectory along the z-axis.

Fig. 4. The relation between the transmission of ions through the SPIG and the RF electric voltage V_{rf}. a) Experimental values: The black circle shows ion current to the Farady cup, for V_m = 10 V, V_g = 15 V and $\omega/2\pi$ = 4.721 MHz. The current to the skimmer is also shown with the white circle. b) Calculated values: The transmission efficiency from the simulation for the case of O_2^+ ion with initial energy, E_i = 3kT/2 (thermal) + 5 eV (translational) and the energy of gas drift $E_{gd}(z)$ = 0.01 eV (3kT/2 = 0.1 eV).

Fig. 5. The experimental curve of the yield (black circle) after the SPIG vs. the voltage difference between the SPIG and the Farady cup for the case of V_{rf} = 60 V and $\omega/2\pi$ =

4.721 MHz. The differential of the curve (dotted line) indicates that the kinetic energy distribution of ions at the end of the SPIG is about 0.8 eV(FWHM).

Fig. 6. The characteristics of cooling (black circle) and focusing (inset) in the SPIG calculated under the same conditions as in Fig. 4(b) except for V_{rf} = 60 V. These curves are the average for 200 ions.

Fig. 7. The distributions of kinetic energy E (white circle) and position r (black circle) of the ions at the end of the SPIG. This is calculated under the same conditions in Fig. 6.

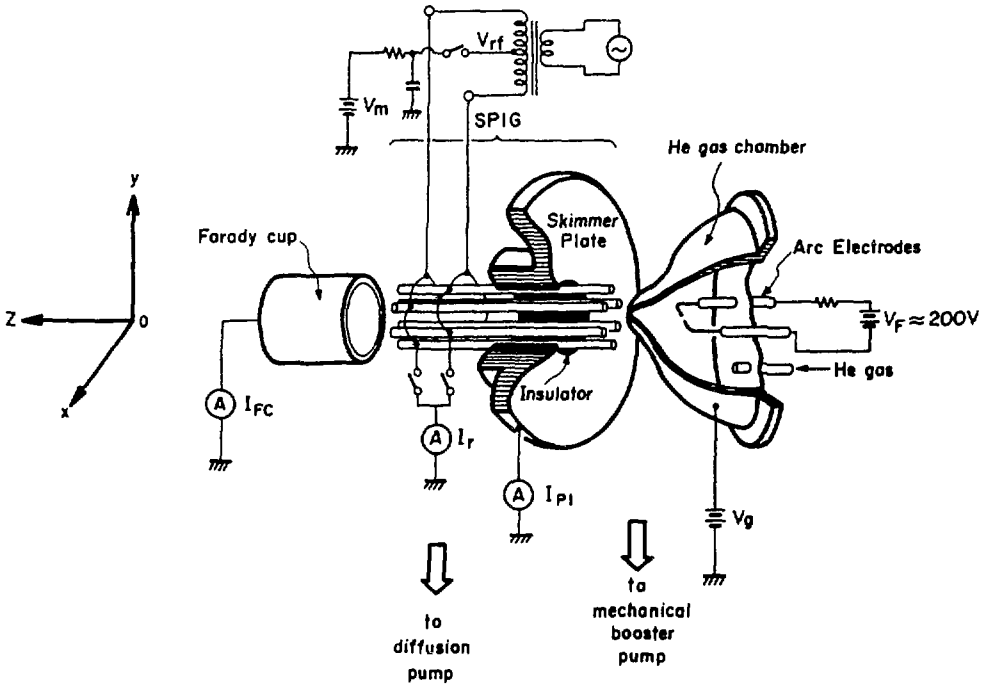
y
Z
0
x
Vrf
Vm
SPIG
He gas chamber
Faraday cup
Skimmer Plate
Arc Electrodes
$V_F \approx 200V$
He gas
Insulator
I_{FC}
I_r
I_{PI}
Vg
to diffusion pump
to mechanical booster pump

Fig. 1

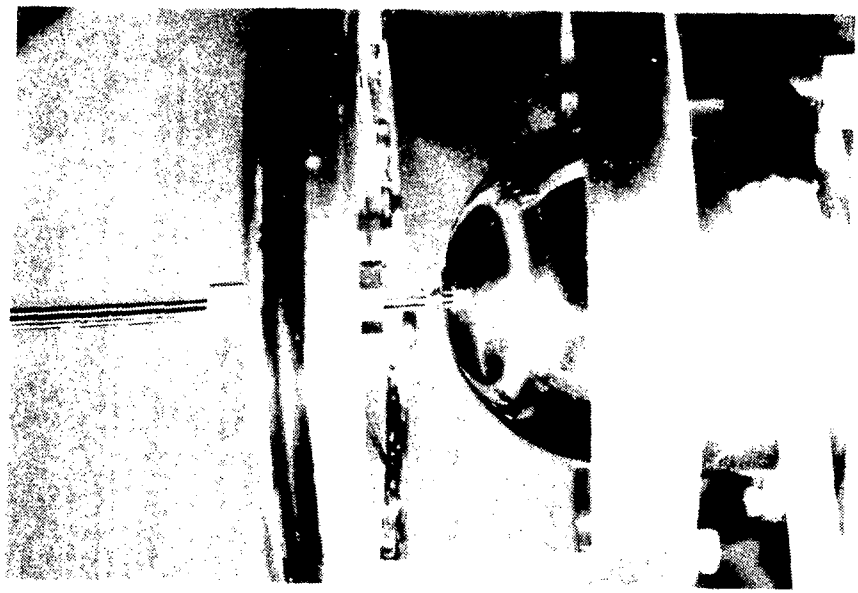

Fig. 2

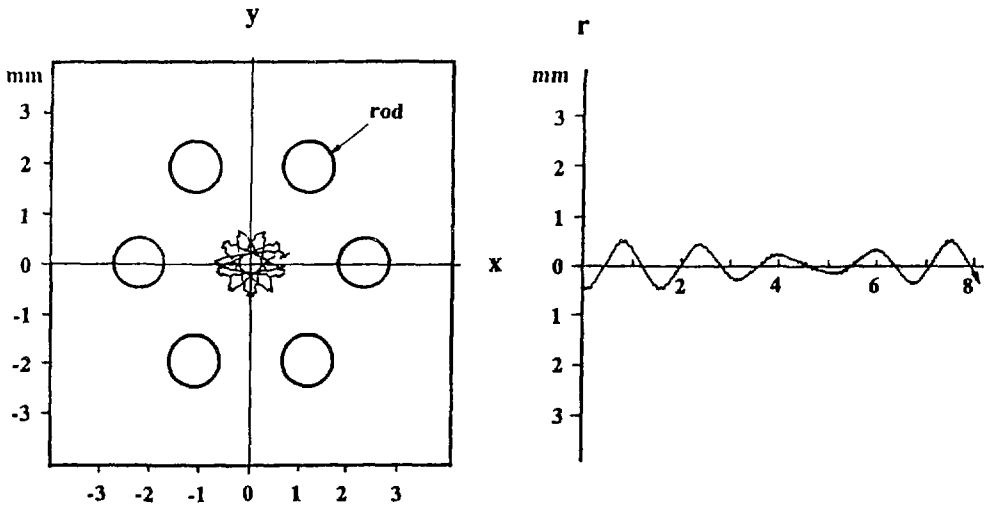

Fig. 3

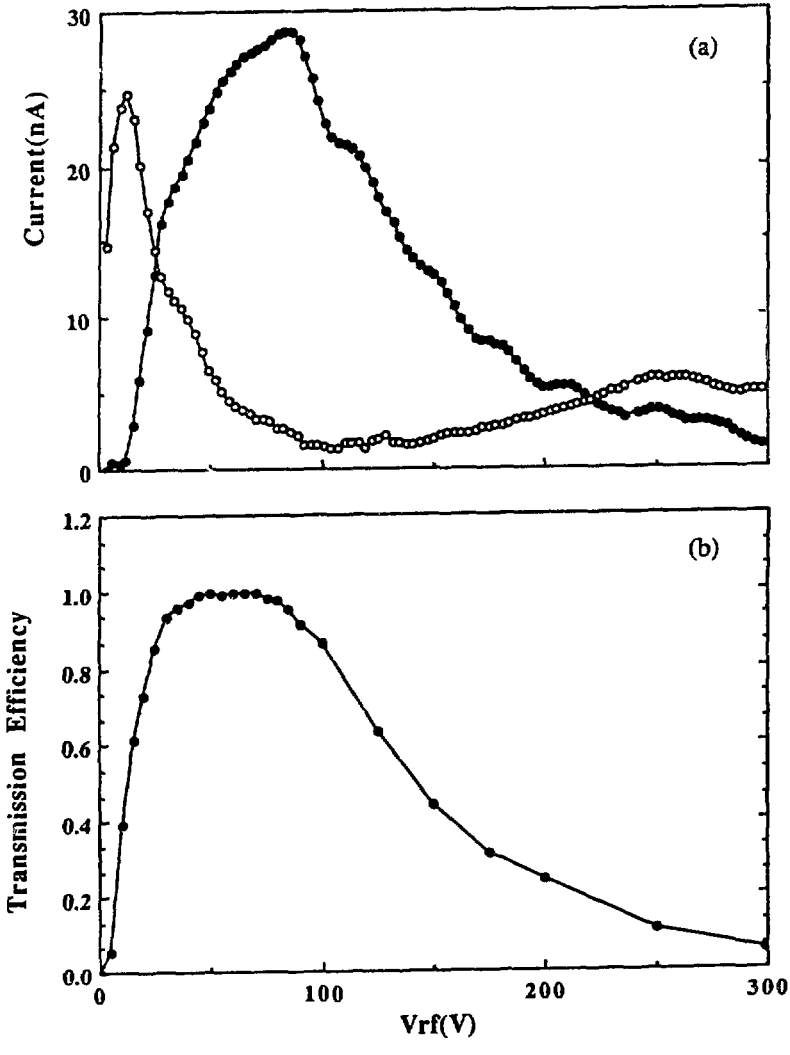
(a)
Current(nA)
30
20
10
0
(b)
Transmission Efficiency
1.2
1.0
0.8
0.6
0.4
0.2
0.0
0
100
200
300
Vrf(V)

Fig. 4

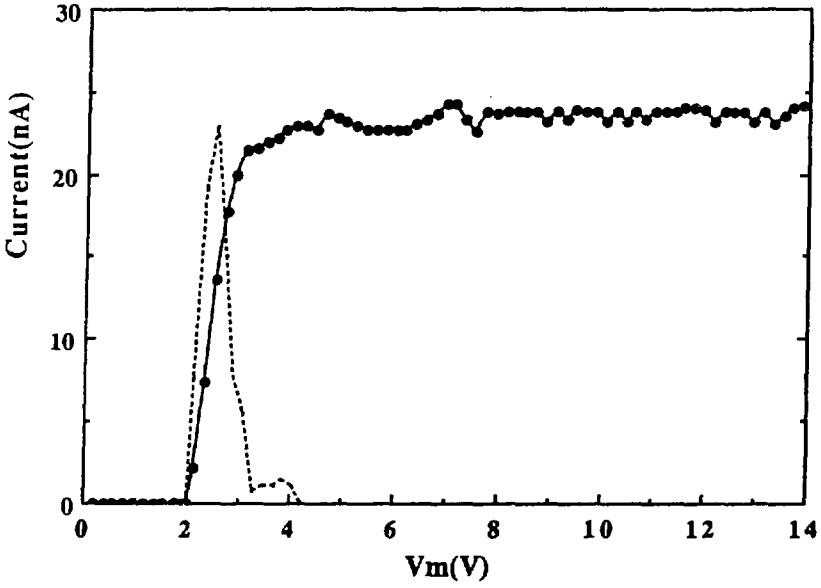

Fig. 5

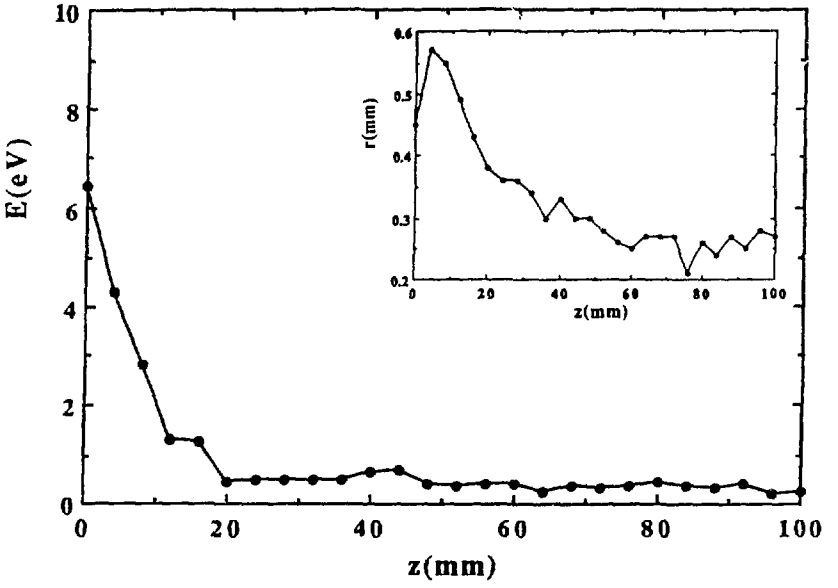

Fig. 6

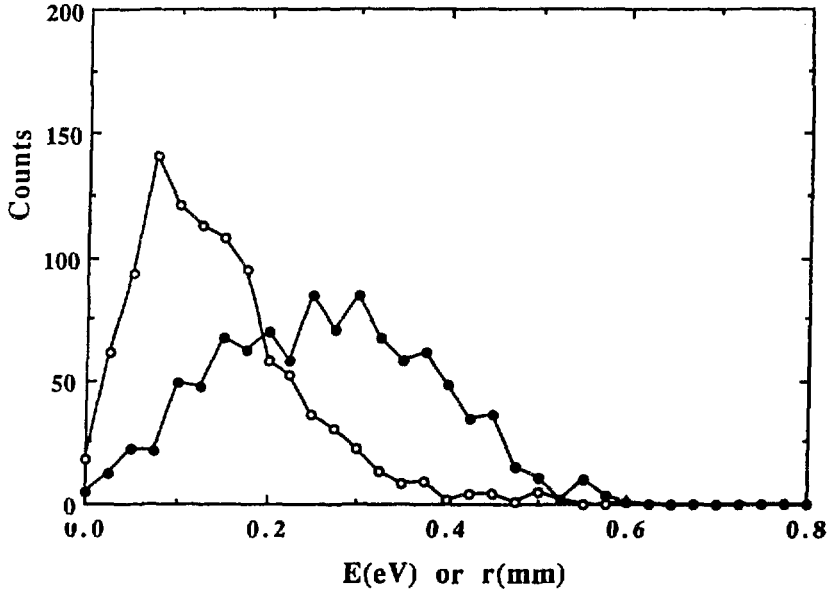

Fig. 7